Journal of Molecular Catalysis A: Chemical 299 (2009) 68–76

Contents lists available at ScienceDirect

Journal of Molecular Catalysis A: Chemical

journal homepage: www.elsevier.com/locate/molcata

Hydroisomerization of n-heptane on the $Pt/H_3PW_{12}O_{40}$/Zr-MCM-41 catalysts

J.A. Wang[a,*], X.L. Zhou[c,**], L.F. Chen[a], L.E. Noreña[b], G.X. Yu[d], C.L. Li[c]

[a] Escuela Superior de Ingeniería Química e Industrias Extractivas, Instituto Politécnico Nacional, Col. Zacatenco, 07738 México, D.F., Mexico
[b] Departamento de Ciencias Básicas, Universidad Autónoma Metropolitana-A, Av. San Pablo No. 180, 02200 México, D.F., Mexico
[c] Petroleum Processing Research Center, East China University of Science and Technology, 200237 Shanghai, China
[d] School of Chemistry and Environmental Engineering, Jianghan University, 430056 Wuhan, China

ARTICLE INFO

Article history:
Received 16 March 2008
Received in revised form
25 September 2008
Accepted 1 October 2008
Available online 17 October 2008

Keywords:
Hydroisomerization
n-Heptane
Acidic catalyst
Mesoporous materials
Heteropolyacid
Zr-MCM-41

ABSTRACT

Catalytic properties of the 1 wt.%Pt/25 wt.%$H_3PW_{12}O_{40}$/Zr-MCM-41-n (designated as Pt/HPW/WSZn, where n = Si/Zr = 25, 15, 8, 4, respectively) catalysts were evaluated in a microreactor system for the hydroisomerization of n-heptane at atmospheric condition. Catalytic results show that tungstophosphoric acid promoted mesoporous Pt/Zr-MCM-41 catalysts have potential important for the commercialization of n-heptane isomerization due to their high activity and unique selectivity to multibranched isoheptanes. It was found that 2-methylhexane was predominant in the monobranched isoheptanes and 2,3-dimethylpentane was the prevailing compound in the multibranched products. In the cracking products, only butane (isobutane and n-butane) and propane were formed. The formation of the multibranched isoheptanes had a close correlation with the mesopore diameters of the catalysts. The isomerization selectivity could be expressed by a parameter S_P, which is defined as a comprehensive function of Brönsted acid density, metal dispersion and geometry of the catalysts. The reaction mechanisms involving the formations of monobranched and multibranched isoheptanes as well as cracking products were discussed and postulated.

1. Introduction

The isomerization of n-alkanes to i-alkanes is one of the most important and economical catalytic processes in the petroleum refining industry. In this process, the straight chain alkanes are transformed into branched isomers boosting research octane number (RON) to improve the gasoline fuel quality. For example, the RON of n-heptane is 0, whilst, it raised up to 56, 92 and 120 for 3-methylhexane, 2,3-dimethylpentane and toluene, respectively.

Previous investigations have predominantly concentrated on the isomerization of n-pentane and n-hexane [1–7]; these processes were successfully commercialized in the last century. Unfortunately, the hydroisomerization of heavier hydrocarbons like n-heptane has not yet been commercialized [8–11]. The skeletal isomerization of n-heptane to isoheptane is rather difficult to be controlled and the cracking reactions through β-scission of C_7-carbenium ion intermediates on acidic sites, leading to low selectivity for di- and tri-branched isomers [12]. The cracking ability is more significantly exhibited for the hydrocarbons having long carbon chain, for example, reaction conditions that may selectively isomerize n-C_6 over zeolite catalysts would almost exclusively produce cracking products for n-C_8 [13]. This is one of the reasons why industrial isomerization is limited to C_4 and C_5/C_6 feedstock up to date. Investigation of heavier n-alkanes (including n-heptane) isomerization for the production of more amounts of reformate gasoline fuel is therefore very important and challenging.

It is well known that the hydroisomerization of C_5/C_6 is usually carried out on a bifunctional catalyst, consisting of a protonating acid and a metal function. According to the traditional mechanism, the noble metal catalyzes hydrogen transfer reactions (hydrogenation/dehydrogenation), while the isomerization and cracking of the hydrocarbon skeletons are performed on Brönsted acid sites. For a satisfactory catalyst, the metal and the acid functions must be well balanced. It was reported that the current industrial catalysts for C_5/C_6 isomerization like Pt/mordenite was not an ideal catalyst for n-heptane isomerization, because of strong diffusion limitations to di- and tri-branched isoheptane products due to the small dimension of 12 membered-ring pores in mordenite, around 0.65 nm in diameter, which results in significant cracking reactions and thus lowering the isomerization selectivity [14]. Chica and Corma studied the hydroisomerization of n-heptane by using 11 different zeolites-containing catalysts including USY, BETA, SAPO-5 and

* Corresponding author at: Laboratorio de Catálisis y Materiales, ESIQIE, Instituto Politecnico Nacional, Col. Zacatenco, 07738 México, D.F., Mexico.
Tel.: +52 55 57296000x55261; fax: +52 55 55862728.
** Corresponding author.
E-mail addresses: jwang@ipn.mx, wang_j_a@yahoo.com (J.A. Wang), xiaolong@ecust.edu.cn (X.L. Zhou).

1381-1169/$ – see front matter © 2008 Elsevier B.V. All rights reserved.
doi:10.1016/j.molcata.2008.10.016

mordenite, etc. as support, and they claimed that none of these zeolites is adequate for producing a high-octane C_7 isomerate, because the i-C_7 products were predominantly composed of monomethyl compounds with very small amount of dimethylpentane and no trimethylbutane were formed [15].

Some authors concluded that the transport properties of the reactants in the catalysts channels are the most important parameter controlling the final catalyst selectivity [16]. In this decade, researchers and industrialists paid more attention to isomerization of n-heptane and novel solid acid catalysts with large pore diameter including mesoporous molecular sieves in order to develop new generation catalysts for the isomerization of heavier hydrocarbons [17,18]. The isomerization of heavier hydrocarbons currently encounters a technical neck-bottle in obtaining high molar ratio of multibranched to monobranched isomers in the products.

In a previous work, our group reported a tungstophosphoric acid promoted mesoporous Pt/Zr-MCM-41 catalysts showing high catalytic activity for n-heptane isomerization with unique selectivity to multibranched isoheptanes [19]. The molar ratio of multibranched to monobranched isoheptanes in the isomer products varies within a very narrow range between 0.8 and 1.2, which is several times greater than that reported in the literature at similar reaction conditions using zeolites supported catalysts. It may be regarded as an important advancement in the isomerization of heavier hydrocarbons. In the preparation of these catalysts, tetraethylorthosilicate (TEOS) was used as Si precursor. In order to reduce the synthetic cost, we tried to use cheap chemical, fumed silica, as Si precursor to replace TEOS, a series of Zr-modified MCM-41 mesoporous solids were also obtained. The cost of catalyst using fumed silica was reduced to half of that using TEOS. The results of synthesis and structural characterization of Zr-modified MCM-41 materials using fumed silica as Si source and the Pt loaded catalysts were reported [20].

The present work follows the first part published in Refs. [19,20]. The catalytic behaviours of a series of 1 wt.%Pt/25 wt.% $H_3PW_{12}O_{40}$/Zr-MCM-41-n catalysts prepared using fumed silica as Si precursor for the hydroisomerization of n-heptane under atmospheric condition were studied. The catalytic activity and selectivity of these catalysts were comparatively examined in order to correlate the catalyst properties with the surface acidity, metal dispersion and pore geometry. The product distributions were also analyzed in detail to elucidate the possible isomerization mechanisms and the cracking pathways.

2. Experimental

2.1. Synthesis of Zr-MCM-41 and catalysts

The Zr-based mesoporous molecular sieves were prepared by using cationic surfactant cetyltrimethylammonium chloride as synthetic template, zirconium-n-propoxide (70% in propanol) as zirconium precursor and fumed silica as Si source. The detail synthesis information of the support can be seen in the first part of the work [20]. The obtained solids Zr-MC-41-n prepared are sometimes referred to as WSZn (n = Si/Zr = 25, 15, 8 and 4).

The 1 wt.%Pt/25 wt.%$H_3PW_{12}O_{40}$/WSZn catalysts were prepared by a two-step impregnation method. Firstly, the Zr-MCM-41 samples were impregnated with 20 ml of a methanol solution containing a given amount of $H_3PW_{12}O_{40}$ (designated as HPW hereafter). The solvent was entirely removed at 40 °C in a vacuum evaporator and the 25 wt.%HPW/Zr-MCM-41 solids were then impregnated with 20 ml of a water solution containing H_2PtCl_6. A 1 wt.% Pt dried sample was obtained after the solvent was evaporated at 80 °C in an evaporator under vacuum condition. It was noted that the *Kiggen* structure of the pure or dispersed heteropolyacid $H_3PW_{12}O_{40}$ would be decomposed at around 600 °C [21,22]. To avoid any possible decomposition or structural degradation, the 1 wt.%Pt/25 wt.%$H_3PW_{12}O_{40}$/Zr-MCM-41-n catalysts were set to calcination at 300 °C in air for 2 h. The 1 wt.%Pt/25 wt.%$H_3PW_{12}O_{40}$/Zr-MCM-41-n catalysts were designated as Pt/HPW/WSZn.

2.2. Hydrogen chemisorption isotherms

The metal dispersion of the Pt/HPW/WSZn catalysts was measured in a TPD/TPR 2900 analyzer (Micromeritics). 0.2 g of solid sample was placed in a U-type quartz tube and was thermally treated at 300 °C for 1 h under a 99.9% He stream at a rate of 40 ml/min to purge off the adsorbed species. The sample was reduced with hydrogen at that temperature for 2 h. Once again, 99.9% He current was introduced to remove any adsorbed molecular hydrogen on the sample during the reduction. Afterwards, the temperature of the sample was cooled down to 25 °C under the He stream, followed by introduction of a mixture of 10% H_2–90% Ar for hydrogen adsorption. The volume of adsorbed hydrogen was measured to calculate the Pt metal dispersion and particle size by suggesting that a hydrogen atom was chemisorbed by one Pt metal atom under the experimental condition.

2.3. Measurement of N_2 adsorption–desorption isotherms

The specific surface area, pore volume and pore size distribution of the samples were measured with a Digisorb 2600 equipment by low temperature N_2 adsorption–desorption isotherms. Before the measurement, the sample was evacuated at 350 °C. The surface area was computed from these isotherms by using the multi-point Brunauer–Emmett–Teller (BET) method based on the adsorption data in the partial pressure P/P_0 range from 0.01 to 0.2. The value of 0.1620 nm^2 was taken for the cross-section of the physically adsorbed N_2 molecule. The mesopore volume was determined from the N_2 adsorbed at a P/P_0 = 0.4. The pore diameter and pore volume were determined by using the (BJH) method. In all cases, correlation coefficients above 0.99 were obtained.

2.4. Surface acidity measurement

To evaluate and analyze the strength and type of the acid sites, pyridine adsorption on the samples was performed on a 170-SX Fourier-transform infrared (FTIR) spectrometer in the temperature range between 25 and 400 °C. Before pyridine adsorption, the samples were heated to 400 °C in a vacuum, and then cooled to room temperature. Afterwards, the solid wafer was exposed to pyridine, by breaking, inside the spectrometer cell, a capillary-containing 50 μl of liquid pyridine. The IR spectra were recorded at various conditions by increasing the cell temperature from 25 to 400 °C. The number of Brönsted and Lewis acid sites was calculated according to the integral area of the bands at 1540 and 1450 cm^{-1}, respectively.

2.5. Catalytic evaluation for n-heptane hydroisomerizaton

The catalytic reactions for n-heptane isomerization were carried out in a down-flow fixed-bed U-shape reactor (i.d. = 1 cm, 20 cm in length) in the presence of hydrogen at atmospheric conditions. 0.2 g catalyst was loaded and the H_2/n-heptane molar ratio was 12. The liquid n-heptane was placed in a glass saturator with a water bath to control the temperature. Hydrogen (99.9%) passed through it at a flow rate of 40 ml/min and brought the n-heptane feed into the reactor with a partial pressure of 0.077 atm. The reaction temperature was varied from 200 to 320 °C with a programmed temperature

control system at a heating rate of 5 °C/min. The weight hourly space velocity (WHSV) was 3.78 h^{-1}. Before the reaction, platinum on the catalysts was reduced with hydrogen for 2 h at 300 °C.

The products were analyzed using an on-line analytical system (GC Varian3300) equipped with a flame ionization detector (FID) and a HP-PONA 50 m × 0.2 mm capillary column maintained at 30 °C. The temperature of the FID detector was 300 °C.

In n-heptane isomerization reactions, the experimental data were recorded after being stabilized for 5 min at each reaction temperature. It has been proved that neither external nor internal diffusion gave impact on the reactions in this experimental system. The catalytic activity was expressed as n-heptane conversion (C_h) and the isomerization selectivity (S_i) is noted as the sum of all the isoheptanes relative to all the products. The yield of the product *i* (y_i) was calculated according to $y_i = S_i \times C_h$.

3. Results

3.1. Physicochemical properties of the WSZn support and Pt/HPW/WSZn catalysts

The physicochemical properties including the surface feature and crystalline structure of the support characterized by X-ray diffraction (XRD), high resolution transmission electron microscopy (TEM), *in situ* FTIR, solid-state nuclear magnetic resonance (^{31}P-MAS-NMR) and ultraviolet–visible spectroscopic (UV–vis) techniques can be seen in detail in the previous work [20]. In order to bridge these with their catalytic properties which will be reported in this work, a brief description of the physicochemical properties of the WSZn support and Pt/HPW/WSZn catalysts is given herein. The WSZn solids showed mesoporous structures with type MCM-41, having wormhole-like pore packing. The mean pore diameter of the WSZn samples varied with the Si/Zr molar ratio: it increased from 2.2 to 2.5, 2.9 and 3.7 nm when the Si/Zr molar ratio decreased from 25 to 15, 8, and 4, respectively. Increasing the zirconium content led to the pore diameter increasing but the surface area decreasing. These observations indicate that zirconium incorporation strongly affects the textural properties of the resultant materials. The increase in pore diameter with increasing zirconium content suggests that the Zr ions are indeed inserted into the silica framework, which is also supported by UV–vis and NMR characterization [20].

The textural properties of the Pt/HPW/WSZn catalysts were also studied by N_2 adsorption–desorption isotherms method. The loops of N_2 adsorption–desorption isotherms and corresponding pore size distributions were shown in Figs. 1 and 2, and the related textural data of the catalysts were reported in Table 1. The N_2 adsorption–desorption isotherms belong to type IV profiles. The sharp step at P/P_0 relative pressures between 0.2 and 0.4 revealed uniform mesoporous features of the solids. The shape and the sharpness of the isotherms varied with the zirconium content. As the zirconium content in the materials increased, the sharpness of the second stage gradually decreased. The surface area of the catalysts diminished from 549.2 m^2/g to 496.1, 402.5 and 395.3 m^2/g when the Si/Zr molar ratio in the support decreased from 25 to 15, 8 and 4. Compared with the bare support, the surface area of Pt/HPW/WSZn catalysts is significantly decreased; the average pore diameter, however, was obviously increased by approximately 80–120%. It is expected that after impregnation with heteropolyacid, the surface area shows a decrease due to some area being covered by the heteropolyacid species. On the other hand, it is possible for the heteropolyacid to locate at the inner surface of the support pores, because of the diameter of the $H_3PW_{12}O_4$ molecule (approximately 1.2 nm) smaller than that of the average mesopore size (4.8–6.9 nm) of the catalysts, which usually leads to a decrease of the pore diameter. However, in our catalyst system, an increase in pore diameter was found for all the catalysts. This is because the data reported in Table 1 is the average of pore diameters, as shown in Figs. 1 and 2, all the Pt/HPW/WSZn catalysts had a bimodal pore diameter distribution in the mesoporous range, the one between 2.5 and 3.0 nm was the major, along with a minor at the diameter range around 3.6–4.0 nm. These catalysts were prepared by a two-step approach, after thermal treatment, reduction and calcination, some of the pore structures may have collapsed to produce larger ones, leading to an increase in average pore diameter with respect to the bare support. Appearance of the peak centred around 3.6–4.0 nm indicates that two neighbour pores have probably merged by collapsing their co-shared pore wall. In addition, it

Table 1
Textural properties of the Pt/HPW/WSZn catalysts.

Si/Zr	Surface area (m^2/g)	Average pore diameter (nm)	Pore volume (cm^3/g)
25	549.2	4.8	0.800
15	496.1	5.7	0.794
8	402.5	6.1	0.639
4	395.3	6.9	0.518

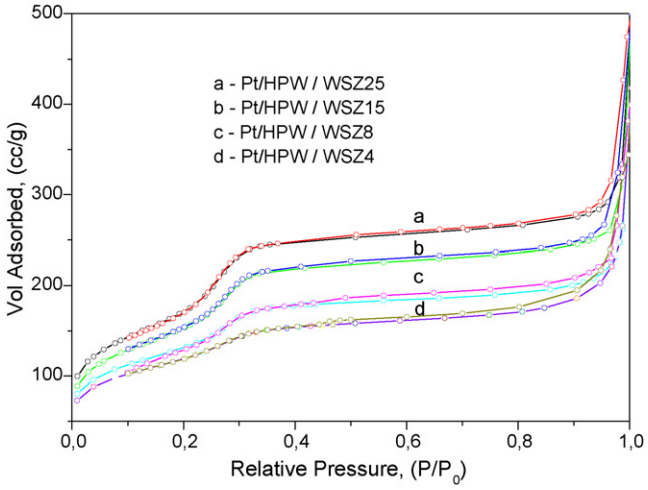

Fig. 1. Loops of N_2 adsorption–desorption isotherms of the Pt/HPW/WSZn catalysts.

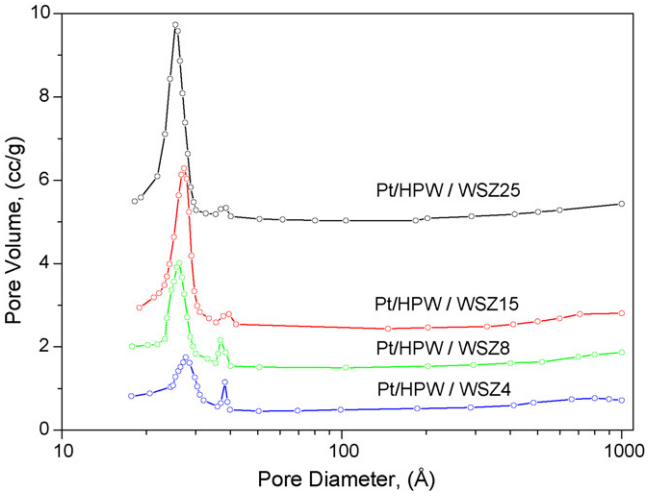

Fig. 2. Pore diameter distributions of the Pt/HPW/WSZn catalysts.

Table 2
Comparison of acid properties of the WSZn support and Pt/HPW/WSZn (n = 25, 15, 8, 4) catalysts. The acid data are calculated with respect to the IR spectra of pyridine adsorption recorded at 100 °C.

Si/Zr	Brönsted acid sites (μmol/g)		Lewis acid sites (μmol/g)		Total acid sites (μmol/g)	
	WSZn	Pt/HPW/WSZn	WSZn	Pt/HPW/WSZn	WSZn	Pt/HPW/WSZn
25	9	135	219	225	228	360
15	55	171	203	229	258	400
8	56	182	165	241	221	423
4	137	191	237	290	374	481

seems that the average pore diameter of the catalysts are larger than that obtained from the two peaks shown in Fig. 2, this is because there are some pores with diameter around 100 nm were formed, which should be related to inter particles voids. In order to show the real textural property of the catalysts, the data of average pore diameter reported in Table 1 included the contribution of the macropores although they are not the predominant.

3.2. Acidity comparison of the WSZn support and Pt/HPW/WSZn catalysts

The surface acidity data of the WSZn support and Pt/HPW/WSZn *catalysts* calculated at room temperature were reported [20]. For hydrocarbon hydroisomerization, the Brönsted acidity at 100 °C is more interesting and is usually used for correlation with the catalytic properties. To better explain the catalytic activity and selectivity of the catalysts, Table 2 gave the surface acidity data of the various WSZn samples and Pt/HPW/WSZn catalysts at 100 °C. For the bare support WSZn solids, the Brönsted acidity linearly increased as the zirconium content increased. In comparison with the pure Zr-MCM-41 support, the surface acidity of the Pt/HPW/WSZn catalysts has great changes: both, the number of the Lewis and Brönsted acid sites were greatly increased after heteropolyacid $H_3PW_{12}O_4$ impregnation, for example, for the catalyst Pt/HPW/WSZ-25, Brönsted acid sites are 135 μmol/g after thermal treatment at 100 °C, which is approximately 15 times greater than those of the bare WSZ25 support, on which only 9 μmol/g Brönsted acid sites are presented. It is also noteworthy that the acidity strength was significantly improved after $H_3PW_{12}O_{40}$ impregnation, for example, the Zr-MCM-41 support samples usually lose their acidity after thermal treatment at 200 °C, which is lower than that the typical reaction temperature required for the isomerization of heavier hydrocarbons; however, in the Pt/HPW/WSZn catalysts, the acidity can be retained at 400 °C, which is higher than the reaction temperature required.

3.3. Catalytic activity

The n-heptane hydroisomerization activities over the 1 wt.%Pt/25 wt.%HPW/WSZn (n = 25, 15, 8 and 4) catalysts in the temperature range between 220 and 320 °C were presented in Fig. 3. It was seen that n-heptane conversion linearly increased with increasing reaction temperatures and the highest conversion for n-heptane appeared for the Pt/HPW/WSZ8 catalyst at all conversion levels.

It was observed that the catalytic activity does not follow the surface acidity variation that was clearly determined by zirconium content. For example, the number of Brönsted acid sites on the catalysts increased from 135 μmol/g to 171, 182 and 191 μmol/g for the catalysts with Si/Zr molar ratio of 25, 15, 8 and 4, respectively, but the highest catalytic activity appeared on a catalyst with Si/Zr ratio of 8. There is a lack of correlation between the surface acidity and their catalytic activity, indicating more activity-determining factors including textural properties, metallic function and others.

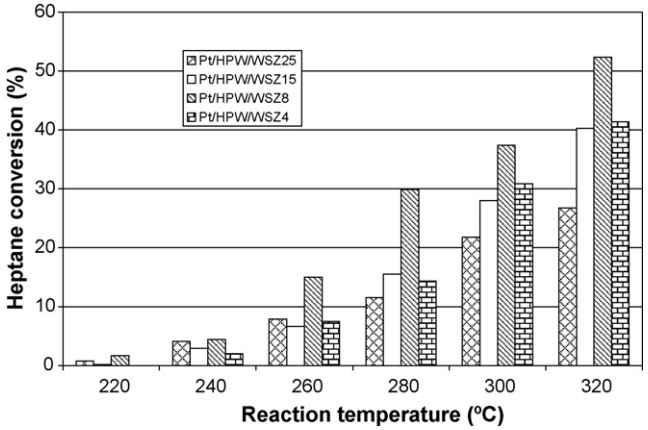

Fig. 3. The n-heptane conversion on the Pt/HPW/WSZn catalysts.

3.4. Isomerization selectivity

Fig. 4 showed the n-heptane isomerization selectivity behaviours over the Pt/HPW/WSZn catalysts. At a low reaction temperature, the selectivity for isoheptanes reached 100%; whilst it diminished by increasing reaction temperatures. The Pt/HPW/WSZ8 catalyst exhibited the highest isoheptanes selectivity with the best catalytic activity at temperatures below 300 °C. In the optimal reaction temperature ranging from 280 to 300 °C, the isomerization selectivity decreased in the order of:

$$\text{Pt/HPW/WSZ8} > \text{Pt/HPW/WSZ4} > \text{Pt/HPW/WSZ15} > \text{Pt/HPW/WSZ25} \quad (1)$$

It is well known that the Brönsted acidities have significant influence on the selectivity of the catalysts. In the present work, the Brönsted acidities of these catalysts diminished in a different order

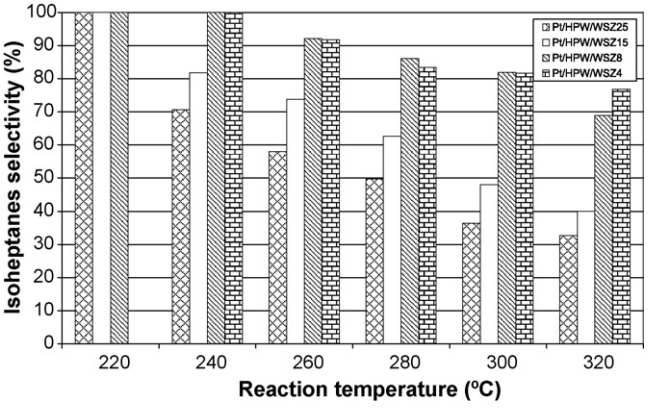

Fig. 4. Isoheptanes selectivity over each Pt/HPW/WSZn catalysts.

Table 3
Selectivity of the various lump products over the Pt/HPW/WSZ25 catalyst.

Temp. (°C)	$S_{iso\text{-}C7}$ (%)	Selectivity (%)			
		Mono-iC_7	Multi-iC_7	$\sum C_3+C_4$	$\sum$others
220	100.0	52.1	47.9	0	0
240	70.6	39.1	31.5	29.4	0
260	57.9	31.9	26.0	42.1	0
280	49.7	26.9	22.8	50.3	0
300	36.5	18.0	18.5	63.5	0
320	32.7	16.3	16.4	67.3	0

as:

$$\text{Pt/HPW/WSZ4 (191 μmol/g)} > \text{Pt/HPW/WSZ8 (182 μmol/g)} > \text{Pt/HPW/WSZ15 (171 μmol/g)} > \text{Pt/HPW/WSZ25 (135 μmol/g)} \quad (2)$$

It was seen, from above orders, that the Pt/HPW/WSZ4 possessed the most number of Brönsted acid sites, but its selectivity for isoheptanes was lower than that of the Pt/HPW/WSZ8 catalyst. Even the surface area is considered, similar results for the density of Brönsted acid sites (number of Brönsted acid sites per surface area unit) were also observed as shown in the following order:

$$\text{Pt/HPW/WSZ4 (4.45 μmol/m}^2\text{)} > \text{Pt/HPW/WSZ8 (4.21 μmol/m}^2\text{)} > \text{Pt/HPW/WSZ15 (3.47 μmol/m}^2\text{)} > \text{Pt/HPW/WSZ25 (2.73 μmol/m}^2\text{)} \quad (3)$$

Above results indicate that although the acidity property strongly affects the isomerization selectivity of the catalysts, it is not the sole factor; the isomerization selectivity may be also dependent on other factors, for example, pore diameter of the catalyst, which will be discussed in detail in the following section.

3.5. Product distribution

The selectivity for various lumped products and that for isoheptanes (S-iC_7) on the Pt/HPW/WSZn catalysts were all shown in Tables 3–6. In the C_7 isomerization products 2-methylhexane (2-MH), 3-methylhexane (3-MH), 2,2-dimethylpentane (2,2-DMP), 2,3-dimethylpentane (2,3-DMP), 2,4-dimethylpentane (2,4-DMP), 3,3-dimethylpentane (3,3-DMP) and 2,2,3-trimethylbutane (2,2,3-TMB) were formed. 2-MH was predominant in the monobranched isomers, while 2,3-DMP reached over 50% of the multibranched isomers.

Fig. 5 demonstrated that the multibranched to monobranched C_7 isomers ratio (designated with R) over the Pt/HPW/WSZn catalysts. The R-value was in the range of 0.8–1.2 below 280 °C, and it was towards around 1 at 300 °C. It was noted that the reaction was close to thermodynamic equilibrium from 280 and 300 °C [15]. The high concentration of multibranched C_7 isomers in the products indicated the possibility to produce high quality gasoline fractions through n-heptane isomerization over our Pt/HPW/WSZn catalysts, this is the most value result obtained from the present work.

It was recognized that the adsorbing capability for hydrocarbons increases with increasing molecular branches, while, their diffusivity within the catalysts will decreases [23]. Therefore, formation of the multibranched isomers would often be more difficult than that of the monobranched ones, because they are prone to be cracked within the pore channels. As shown in Fig. 5, the ratio of the multibranched to monobranched isomers, over all the Pt/HPW/WSZn catalysts, changed within a narrow range which was close to thermodynamic equilibrium at higher reaction temperatures and it was much higher than that of other catalysts described in the literature. For example, Pope et al. reported this ratio ranged from 0.2 to 0.5 at different conversions over the Pt/Cl-alumina and Pt/zeolite catalysts [12]. Kinger et al. even claimed impossibilities to obtain a high-octane-number isomerate by n-heptane hydroisomerization on the Pt-containing zeolite catalysts because of much lower ratio of R in the products under a reaction pressure of 20 bar [16]. All of these results revealed the advantages of our Pt/HPW/WSZn catalysts owing to the high selectivity to multibranched isomers.

Table 4
Selectivity of the various lump products over the Pt/HPW/WSZ15 catalyst.

Temp. (°C)	$S_{iso\text{-}C7}$ (%)	Selectivity (%)			
		Mono-iC_7	Multi-iC_7	$\sum C_3+C_4$	$\sum$others
220	100.0	51.7	48.3	0	0
240	81.8	45.8	36.0	11.2	0
260	73.8	40.2	33.6	26.2	0
280	62.6	31.8	31.2	37.4	0
300	48.0	24.0	24.0	52.0	0
320	40.1	20.0	20.1	59.8	0.1

Table 5
Selectivity of the various lump products over the Pt/HPW/WSZ8 catalyst.

Temp. (°C)	$S_{iso\text{-}C7}$ (%)	Selectivity (%)			
		Mono-iC_7	Multi-iC_7	$\sum C_3+C_4$	$\sum$others
220	100.0	45.3	54.7	0	0
240	100.0	50.8	49.2	0	0
260	92.1	46.1	46.0	7.9	0
280	86.1	43.4	42.7	13.9	0
300	82.5	40.6	41.9	18.5	0
320	68.9	33.7	35.2	31.1	0

Table 6
Selectivity of the various lump products over the Pt/HPW/WSZ4.

Temp. (°C)	$S_{iso\text{-}C7}$ (%)	Selectivity (%)			
		Mono-iC_7	Multi-iC_7	$\sum C_3+C_4$	$\sum$others
240	100.0	49.0	51.0	0	0
260	91.8	47.3	44.5	8.2	0
280	83.5	44.1	45.4	16.5	0
300	81.7	41.6	40.1	18.3	0
320	76.8	38.2	38.6	23.2	0

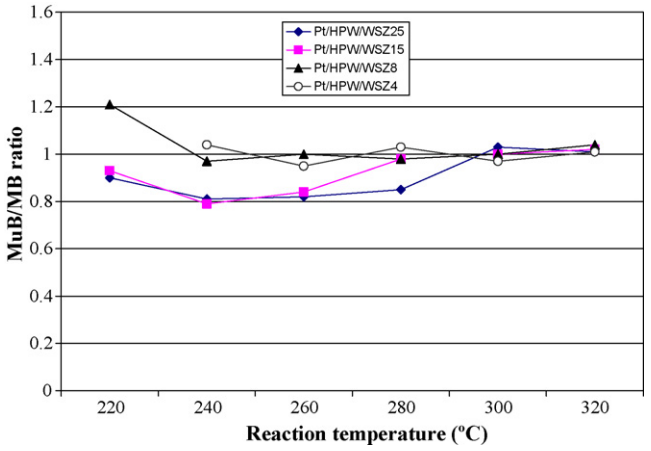

Fig. 5. Multibranched and monobranched isoheptanes ratio for each Pt/HPW/WSZn catalyst vs. the reaction temperature.

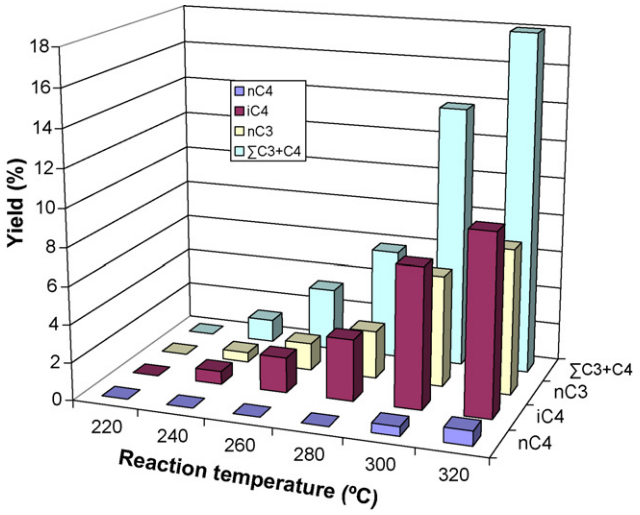

Fig. 6. Yield of cracking products over the Pt/HPW/WSZ25 catalyst.

It was also concluded from our work that the selectivity for multibranched isoheptanes decreased in the order of:

$$(\text{Pt/HPW/WSZ4}, \text{Pt/HPW/WSZ8}) > \text{Pt/HPW/WSZ15} > \text{Pt/HPW/WSZ25} \quad (4)$$

which paralleled to changes in catalyst pore diameter as follows:

$$(\text{Pt/HPW/WSZ4}, \text{Pt/HPW/WSZ8}) > \text{Pt/HPW/WSZ15} > \text{Pt/HPW/WSZ25} \quad (5)$$

These results showed that the pore diameter of the catalysts plays a predominant role in multibranched C_7 formation. Because the multibranched isoheptanes have larger molecular sizes, hence, their formation, desorption and diffusion inside the small pores would be hindered in the zeolites catalysts, which usually results in more cracking products. On the contrary, the present work confirms that multibranched C_7 isomers can be produced on mesoporous molecular sieves supported catalysts.

Figs. 6–9 showed the yields of the cracking products obtained from the Pt/HPW/WSZn catalysts in the temperature range between 220 and 320 °C. It was clear that only n-butane, isobutene and propane were detected in the products. Yields of various cracking products linearly increased with increasing reaction temperatures. It was also seen that n-C_4 was only produced above 300 °C on all the catalysts, while, i-C_4 appeared at the temperature when cracking reactions took place. The isobutane yield was often higher than that of n-C_4, indicating that i-C_4 is probably produced through more than one approaches given in detail in the following section.

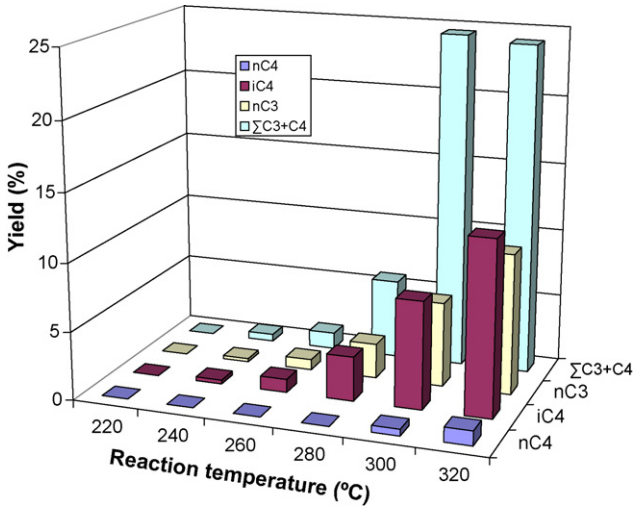

Fig. 7. Yield of cracking products over the Pt/HPW/WSZ25 catalyst.

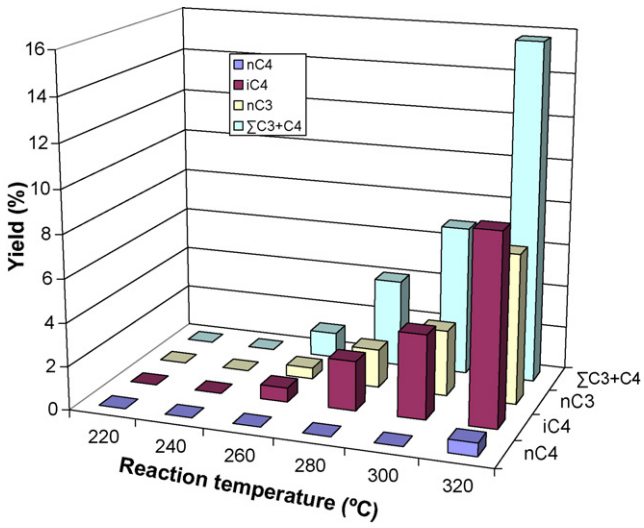

Fig. 8. Yield of cracking products over the Pt/HPW/WSZ25 catalyst.

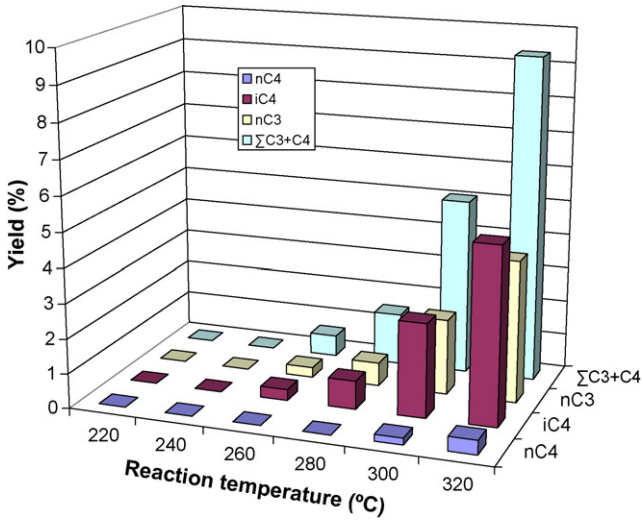

Fig. 9. Yield of cracking products over the Pt/HPW/WSZ25 catalyst.

4. Discussions

4.1. Factors influencing the isomerization selectivity

It has been well known that for a bifunctional catalyst, both the acid function and the metallic function strongly affect the catalytic behaviours according to the traditional mechanism of hydrocarbon isomerization. However, arguments on the factors determining the selectivity appear. Some researchers reported that n-hexane isomerization selectivity might be mainly controlled by the pore structure instead of surface acidity [1]. As shown above, no simple correlation between surface acidity and the isomerization selectivity can be established. This drives us to search for the

Table 7
Comparison of the Brönsted acidity density (D_B), pore diameter (D_p) and Pt dispersion (M_d) and isomerization selectivity parameter (S_P) of the Pt/HPW/WSZn catalysts.

Catalysts	D_B (μmol/m^2)	D_p (nm)	M_d	S_P (10^{-9} μmol/m)
Pt/HPW/WSZ25	0.24	4.8	0.64	0.73
Pt/HPW/WSZ15	0.34	5.7	0.51	1.19
Pt/HPW/WSZ8	0.45	6.1	0.55	1.50
Pt/HPW/WSZ4	0.48	6.9	0.42	1.39

complementary influencing factors for explanation of our experimental results.

For the zeolitic catalysts, the pore geometry of the catalyst plays a very important role in the isomerization reactions. Generally speaking, a small pore diameter of the catalyst is prone to produce more cracking products. In the studies of heavier hydrocarbons isomerization using mesoporous catalysts with ordered pore channels, effect of the geometrical effect of the catalysts on the catalytic behaviours has not been clear yet. To better characterize isomerization selectivity, it is necessary to define a new parameter including all the important related factors. Herein, we define a new parameter S_P, called the isomerization *selectivity parameter* to measure the degree of the isomerization by including three factors: (i) the acid function, (ii) the metal function and (iii) the geometry function of the catalyst. Largely, the effect factors on the isomerization selectivity can be simply lumped into two groups: factors related to reaction conditions and those to the catalyst:

$$S_P = S_{\text{selectivity parameter}} = F_{\text{catalyst}} F_{\text{reaction conditions}} \quad (6)$$

where $F_{\text{reaction conditions}} = f$ (reaction temperature, pressure, space velocity, reaction time, etc.).

The reaction conditions were constant in our experiment; therefore, S_P depends only on the catalyst factor is shown as

$$F_{\text{catalyst}} = f_{\text{acidity}} f_{\text{metal}} f_{\text{geometry}} \quad (7)$$

where f_{acidity} was defined as the Brönsted acid density; f_{metal} was defined as the metal dispersion determined by H_2 chemisorption and the f_{geometry} was simply defined as the pore diameter of the catalysts ignoring the effect of pore shape or channel length because our catalysts have the same pore shape (hexagonal) and similar particle size. It is clear that S_P parameter includes the surface Brönsted acidity which relates to the acid function, the metal dispersion which associates with the metal function or the accessibility of the active metal clusters, as well as the pore diameter which characterizes the geometry function, whilst the surface area has already been expressed in the f_{acidity} term.

In order to verify whether S_P parameter could be used as a criterion in our work, related data for the Pt/HPW/WSZn catalysts have been computed. Applicability of S_P parameter for isomerization selectivity estimation was shown in Table 7. It was seen that the isomerization selectivity diminished in the following order:

$$\text{Pt/HPW/WSZ8} > \text{Pt/HPW/WSZ4} > \text{Pt/HPW/WSZ15} > \text{Pt/HPW/WSZ25} \quad (8)$$

The order (8) was in line with isomerization selectivity behaviours as given in the order (1). Thus the isomerization selectivity of n-heptane over our catalysts is able to be estimated by using parameter S_P. The bigger the S_P value is, the higher the isomerization selectivity should be. However, care must be taken for the geometrical factor in the S_P factor, it only indicates that, in the mesoporous material supported catalysts with ordered pore channels, larger pore diameter may be in favour of enhancement of isomerization selectivity, or be beneficial to the formation of multibranched isomers. S_P factor may be not suitable for oxides containing disordered pore structures. In fact, with respect to the traditional bifunctional mechanism, the only principal new element added to the parameter S_P is the proposal of the strong effect of the geometry of the catalyst. Although S_P is not expected to be a general criterion for prediction the selectivity for various catalyst systems, it, at least, emphasizes the comprehensive effects of the catalysts on the catalytic behaviours in the hydroisomerization reactions. In our catalysts, the Pt/HPW/WSZ4 catalyst has the largest pore diameter and the biggest number of Brönsted acid sites; however, it exhibits smaller surface area thus lower metal dispersion. As a consequence, it has a smaller S_P value (1.39) thus a lower isomerization selectivity in the reaction range between 220 and 300 °C, in comparison with that of the Pt/HPW/WSZ8 catalyst (S_P = 1.50). Above 300 °C, metal dispersion and acidity may be altered and cracking reaction rate is relatively rapid, at such condition, the geometrical factor (pore diameter) plays as a more important role determining the selectivity, smaller size of the pore diameter may result in more cracking products. Hence, the Pt/HPW/WSZ4 catalyst with largest pore diameter exhibits the highest isomerization selectivity at 320 °C.

4.2. C_7 isomers formation

Different mechanisms have been suggested for the isomerization of paraffinic hydrocarbons over metal-supported on solid acid catalysts [24]. Blekkan et al. proposed a novel mechanism *via* metallocyclic intermediates instead of carbenium ions for n-heptane isomerization over an oxygen-modified molybdenum carbide catalyst [25]. This mechanism was based upon the results that isomerization selectivity was independent of the n-heptane conversion and the cracking products contained higher yields of methane and ethane relative to that of C_4 and C_3. Obviously, it could not be accepted to explain our results, because only C_4 and C_3 were presented in the cracking products and the selectivity for isoheptanes varied with the n-heptane conversion in our test. In addition, the heptane isomerization reactions in Blekkan's experiments were carried out at high pressures, whilst an atmospheric pressure was applied in our test. The monobranched isomers were mainly 2-methylhexane and 3-methylhexane, indicating that their formations follow a protonated cyclopropane mechanism [14]. The n-heptane molecules were first adsorbed on the active sites, where the C–H bonds were activated and dehydrogenated by Pt metal clusters to form the primary surface intermediates which converted to carbenium ions with protons on the acid sites and then produced protonated cyclopropane intermediates. It was also observed that 2-methylhaxane was a main product compared to 3-methylhexane. The latter was produced at higher reaction temperatures, indicating 3-methylhexane should be also formed simultaneously through another pathway including the rapid shift of the methyl groups in 2-methylhaxane.

Patrigeon and co-workers reported that in the n-heptane isomerization over H-β zeolite, the yield of monobranched isomers increased with increasing conversion up to a maximum and then decreased while the yield of multibranched isomers went through a maximum at higher conversion [26], thus they believed that the multibranched isomers were the secondary products of the primary products (monobranched isomers). However, such a maximum was not observed in our experiments because multibranched to monobranched isoheptanes ratio (R) varied in a rather narrow range of 0.8 and 1.2 over a wide range of conversion. In one hand, if the rate of monobranched isomers formation is the same as or similar to that of multibranched isomers formation through an approach of further isomerization of the monobranched isomers, then, the R-value should remain unchanged. On the other hand, if both the

multibranched and monobranched isomers are resulted from the same precursors at a same rate, that is to say, they may occur in parallel, sharing a common reaction intermediate, the *R*-value should remain the same. Therefore, in the n-heptane isomerization catalyzed with our mesoporous catalysts, the multibranched isoheptanes might be formed as secondary products of the monobranched isomers through a consecutive reaction pathway or as primary products through reactions in parallel to the formation of the monobranched isomers originated from the same intermediates.

4.3. $C_3 + C_4$ formation

Acidic-catalyzed cracking of paraffinic hydrocarbons on zeolite-supported catalysts were reported [27,28]. However, mechanism on the n-heptanes catalyzed with mesoporous catalysts has not been reported yet. In the present work, the cracking products on Pt/HPW/CSZ8 and Pt/HPW/CSZ4 catalysts were composed of n-butane, isobutene and propane. The cracking reactions took place from moderate to high n-heptane conversion. At low conversion, the isomerization selectivity was 100%, indicating the faster rate of the isomerization reactions compared to that of cracking because the latter required higher active energy for the C–C bond cleavage. The selectivity to butane and propane increased by increasing reaction temperatures at the expense of isomerization selectivity. The cracking mechanisms would be possibly proposed according to the cracking products and their yields.

The n-C_4 was detectable from 280 °C and above temperature on all the catalysts, whilst i-C_4 appeared only at moderate to higher temperature ranges. The isobutane yield was much higher than that of n-C_4. The absence of n-butane at low temperature could be expected if one takes into account the relative stabilities of the starting and final carbocations formed from 2,3-DMP$^+$, 2,2-DMP$^+$ and 2,4-DMP$^+$ intermediates. In the low reaction temperature range, the β-scission of the methylhexyl and dimethylpentyl cations is believed to be mainly responsible for the formation of isobutane and propane.

In the dimethylpentane products, it was seen that the yields of 2,2-dimethylpentane and 2,4-dimethylpentane were quite low compared to that of 2,3-dimethylpentane. It is known that cracking of 2,3-dimethylpentane leads to the formation of n-C_4 + C_3, and the cracking of 2,2-dimethylpentane and 2,4-dimethylpentane leads to the formation of i-C_4 + C_3. In our test, no n-C_4 was detectable at a temperature below 280 °C, these results indicate that the 2,3-dimethylpentane was more stable than 2,2-dimethylpentane and 2,4-dimethylpentane at such temperatures according to reactions (9) and (10). The double C=C bond in isobutene could be further hydrogenated on the metal sites to propane and isobutane as final products.

Reaction (9):

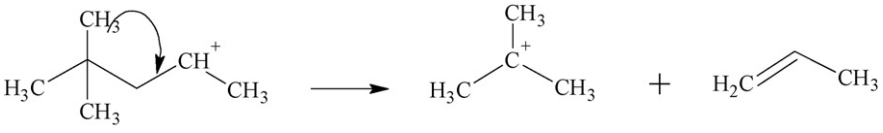

Reaction (10):

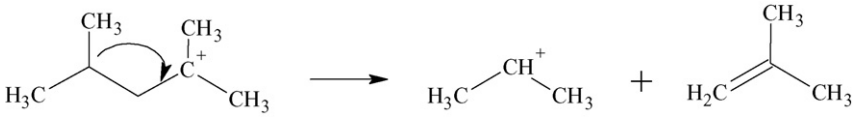

At 280 °C and higher, the formation of n-C_4 indicated the cracking reactions could probably be proceeded through β-scission reactions of 2,3-dimethylpentyl, 2-methylhexyl and 3-methylhexyl pathways through reactions (11)–(13).

Reaction (11): β-scission of 2,3-dimethylpentyl carbenium ions

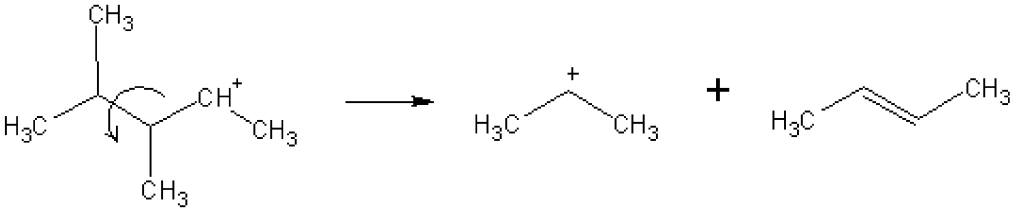

Reaction (12): β-scission pathway of 2-methylhexyl carbenium ions

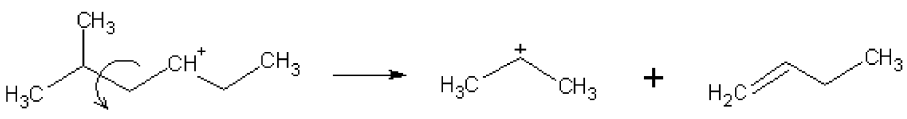

Reaction (13): β-scission of 3-methylhexyl carbenium ions

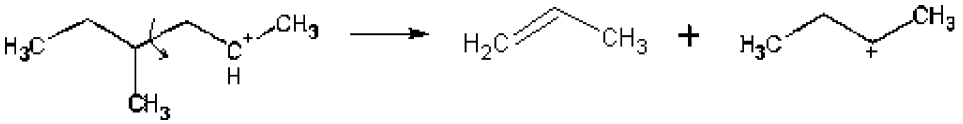

The ratio of multibranched to monobranched isomers varied within a narrow range for different n-heptane conversions and reaction temperatures, indicating similar cracking rate for multibranched and monobranched isomers. Due to the complexity of the reaction system and the possibility of methyl shift in n-C_4^+ to form i-C_4^+, the n-butane yield was often lower than that of i-butane.

5. Conclusions

It has been proven that the Pt/HPW/Zr-MCM-41 catalysts exhibit superior isomerization catalytic properties in the n-heptane hydroisomerization reaction at atmospheric condition. The isomerization selectivity reaches 100% until 260 °C. In the products, 2-methylhexane is dominant in the monobranched isomers and 2,3-dimethylpentane is the main compound accounting for more than 50% of the multibranched products. The formation of multibranched isoheptanes has a close relation with the pore diameter of the mesoporous catalysts. The ratio of multibranched to monobranched isoheptanes varies within a narrow range between 0.8 and 1.2, which is independent of the reaction temperature or conversion and is much higher than zeolite-containing catalysts, showing the superiority of our mesostructured catalysts. This important result reveals the possibility to obtain high-octane-number gasoline by n-heptane hydroisomerization by using mesoporous catalysts.

In the cracking products, only butane (isobutane and n-butane) and propane are detected. The yield of isobutane is higher than n-butane. The former appears in a wide reaction range and the latter is formed only at higher temperatures. They are formed through either β-scission of methylhexyl or dimethylpentyl intermediates.

A new parameter, S_P, defined as the comprehensive function of acidity density, metal dispersion and pore diameter of the catalysts, has been proposed as a criterion to estimate the isomerization selectivity. For the mesoporous catalysts, the bigger the S_P value of a catalyst, the higher the selectivity to isoheptane is.

Acknowledgements

L.F. Chen wishes to acknowledge the scholarship for her study of the doctorate degree offered by the CONACyT-Mexico. The financial support from the projects SIP-IPN-2006067, CONACyT (MEXICO)-NSF (CHINA) J110.234/2007 and China 973 program (Grant No. 2004CB720603) by China Ministry of Science and Technology is greatly appreciated. The authors thank Dr. J.L. Contreras for help in the catalysis evaluation.

References

[1] N. Viswanadham, L. Dixit, J.K. Gupta, M.O. Garg, Journal of Molecular Catalysis A: Chemical 258 (2006) 15.
[2] M.N. Yoshioka, T. Garetto, D. Cardoso, Catalysis Today 107–108 (2005) 693.
[3] N. Vu, J. van Gestel, J.P. Gilson, C. Collet, J.P. Dath, J.C. Duchet, Journal of Catalysis 231 (2005) 468.
[4] M.G. Falco, S.A. Canavese, N.S. Fígoli, Catalysis Communications 2 (2001) 207.
[5] M. Risch, E.E. Wolf, Catalysis Today 62 (2–3) (2000) 255.
[6] R.A. Asuquo, G. Edermirth, J.A. Lercher, Journal of Catalysis 155 (1995) 376.
[7] H. Liu, G.D. Lei, W.M.H. Sachtler, Applied Catalysis A: General 146 (1996) 165.
[8] N. Bouchenafa-Saïb, R. Issaadi, P. Grange, Applied Catalysis A: General 259 (2004) 9.
[9] Z.B. Wang, A. Kamo, T. Yoneda, T. Komatsu, T. Yashima, Applied Catalysis A: General 159 (1997) 119.
[10] J.M. Campelo, F. Lafont, J.M. Marinas, Applied Catalysis A: General 152 (1997) 53.
[11] T. Matsuda, H. Sakagami, N. Takahashi, Catalysis Today 81 (2003) 31.
[12] T.D. Pope, J.F. Kriz, M. Stanciulescu, J. Monnier, Applied Catalysis A: General 233 (2002) 45.
[13] I.E. Maxwell, Catalysis Today 1 (1987) 385.
[14] V.M. Akhnedov, S.H. Al-Khowaiter, J.K. Al-Refai, Applied Catalysis A: General 252 (2003) 353.
[15] A. Chica, A. Corma, Journal of Catalysis 187 (1999) 167.
[16] G. Kinger, D. Majda, H. Vinek, Applied Catalysis A: General 225 (2002) 301.
[17] I. Eswarmoorthi, V. Sundaramurthy, N. Lingappam, Microporous and Mesoporous Materials 71 (2004) 109.
[18] R. Mokaya, W. Jones, G. Poncelet, Catalysis Letters 49 (1997) 87.
[19] J.A. Wang, L.F. Chen, L. Noreña, J. Navarrete, M.E. Llanos, J.L. Contreras, O. Novaro, Microporous and Mesoporous Materials 112 (2008) 61–67.
[20] L.F. Chen, J.A. Wang, L. Noreña, J. Aguilar, J. Navarrete, P. Salas, J.A. Montoya, P. Del Angel, Journal of Solid State Chemistry 180 (2007) 2958.
[21] E. López-Salinas, J.G. Hernández-Cortëz, I. Schifter, E. Torres-García, J. Navarrete, A. Gutiérrez, T. Löpez, P.P. Lottici, D. Bersani, Applied Catalysis A: General 193 (2000) 215.
[22] Q.Y. Liu, W.L. Wu, J. Wang, X.Q. Ren, Y.R. Wang, Microporous and Mesoporous Materials 76 (2004) 51.
[23] V. Fierro, Y. Schuurman, C. Mirodatos, J.L. Duplan, J. Verstraete, Chemical Engineering Journal 90 (2002) 139.
[24] Y. Ono, Catalysis Today 81 (2003) 3.
[25] E.A. Blekkan, C. Pham-Huu, M.J. Ledoux, J. Guille, Industrial and Engineering Chemistry Research 33 (7) (1994) 1657.
[26] A. Patrigeon, E. Benazzi, Ch. Travers, J.Y. Bernhard, Catalysis Today 65 (2001) 149.
[27] S. Tiong Sie, Industrial and Engineering Chemistry Research 32 (1993) 397.
[28] S. Tiong Sie, Industrial and Engineering Chemistry Research 32 (1993) 403.